Journal of the American College of Cardiology Vol. 53, No. 23, 2009

Published by Elsevier Inc.
ISSN 0735-1097/09/$36.00
doi:10.1016/j.jacc.2009.03.033

Skeletal Muscle Microvascular Flow in Progressive Peripheral Artery Disease

Assessment With Continuous Arterial Spin-Labeling Perfusion Magnetic Resonance Imaging

Wen-Chau Wu, PHD,*# Emile Mohler III, MD,† Sarah J. Ratcliffe, PHD,‡ Felix W. Wehrli, PHD,* John A. Detre, MD,*‖ Thomas F. Floyd, MD§‖

Philadelphia, Pennsylvania; and Taipei, Taiwan

Objectives We present the novel application of continuous arterial spin-labeling (CASL) magnetic resonance imaging (MRI) for the measurement of calf muscle perfusion in subjects with progressive peripheral arterial disease (PAD).

Background Peripheral arterial disease is largely considered to be a disease of conduit vessels. The impact of PAD upon microvascular flow in the end-organ, muscle, remains unknown. Continuous arterial spin-labeling is a noninvasive MRI method capable of measuring microvascular flow and might assist in our understanding of the impact of PAD upon the microvasculature.

Methods Forty subjects with varying degrees of PAD and 17 age-matched PAD-free subjects were recruited and underwent measurement of the ankle-to-brachial index (ABI) and CASL. Peak hyperemic flow (PHF) and time-to-peak (TTP) were computed and assessed as a function of ABI and calf muscle group.

Results An ABI dependence was found in both PHF ($p = 0.04$) and TTP ($p < 10^{-4}$). Whereas TTP increased almost immediately with increasing PAD severity, PHF was, in contrast, relatively well preserved until later stages of disease.

Conclusions The CASL flow measurements correlate with disease state as measured by ABI and demonstrate preserved microvascular flow reserve in the presence of early to intermediate vascular disease. (J Am Coll Cardiol 2009;53: 2372–7) © 2009 by the American College of Cardiology Foundation

Peripheral artery disease (PAD) refers to disorders of the circulatory system outside the brain and heart as a consequence of narrowing and/or obstruction of peripheral arteries that carry blood to the extremities (1). Recent studies demonstrate that the atherosclerotic process in lower extremity PAD is not confined to conduit vessels but also affects skeletal muscle flow reserve (2), metabolism (3), endothelial and muscle mitochondrial function (4), gene transcription (5), and apoptosis (6). Several methods have been applied to measure skeletal muscle perfusion, such as positron emission tomography (7), dynamic susceptibility magnetic resonance imaging (MRI) (8), and ultrasound (9), although each involves either ionizing radiation and/or the administration of exogenous contrast agents.

Arterial spin labeling (ASL) (10) is a noninvasive MRI technique that offers quantitative perfusion measurements. A typical ASL experiment comprises 2 scans: the "tag" image is acquired after the protons in arterial blood are "tagged" by radiofrequency pulses, most commonly by inverting the blood proton magnetization, whereas the "control" image is obtained without net magnetization perturbation in arterial blood. Blood flow is then computed from the signal difference between the tag and control images. Currently, the gold standard for measuring perfusion in skeletal muscle is the microsphere experiment (11), which is highly invasive, because it requires arterial injection and subsequent arterial sampling as well as tissue sampling. A comparison study of ASL and microsphere methods (12) has shown a clear agreement in rat leg muscle, whereas ASL offers improved spatial and temporal resolution.

Arterial spin labeling has also been successfully applied to the measurement of blood flow in the extremity muscle of healthy humans (13–16). We present the first attempt to

From the Departments of *Radiology, †Medicine (Vascular Medicine), ‡Biostatistics and Epidemiology, §Anesthesiology and Critical Care, and ‖Neurology, Hospital of University of Pennsylvania, Philadelphia, Pennsylvania; and the #Graduate Institute of Clinical Medicine, National Taiwan University, Taipei, Taiwan.

Dr. Detre is the co-owner of U.S. Patent #6717405—"Arterial spin labeling using time varying gradients"—and has received royalties from the University of Pennsylvania for the licensure of its patent on ASL. This study was supported by the National Institutes of Health grant R01HL075649.

Manuscript received December 2, 2008; revised manuscript received February 24, 2009, accepted March 10, 2009.

employ a continuous version of arterial spin labeling (CASL) to measure calf muscle perfusion in subjects with various degrees of PAD.

Methods

Subjects and MRI. The Institutional Review Board approved the study protocol, and written consent was obtained from all subjects. A cohort of 40 subjects diagnosed with PAD and 17 age-matched PAD-free subjects were recruited in this study (age 26 to 86 years, 24 women and 33 men).

Subjects first underwent measurement of ankle-to-brachial index (ABI). An ABI between 0.90 and 1.30 is generally considered to be normal, with an ABI between 0.90 and 1.00 indicating borderline PAD; an ABI between 0.50 and 0.90 can represent a wide range of moderate disease, and an ABI below 0.50 usually indicates severe PAD (17). Therefore we defined 4 clinical categories of ABI in the following manner: category 0: $0.90 \leq$ ABI ≤ 1.30; category 1: $0.70 \leq$ ABI < 0.90; category 2: $0.50 \leq$ ABI < 0.70; and category 3: ABI < 0.50. We then stratified subjects accordingly. Fourteen of the subjects in category 0 were also included in a previous study (16).

The MRI was conducted on a 3.0-T Siemens Trio system (Erlangen, Germany) with a transmit/receive knee coil (Nova Medical, Inc., Wakefield, Massachusetts). Subjects were imaged supine. A single-slice version of the CASL sequence was used (18) with a single-shot gradient-echo echoplanar readout: field-of-view = 22 cm, in-plane matrix size = 64 × 64, slice thickness = 1 cm, repetition time = 4 s, echo time = 17 ms, flip angle = 90°, tagging duration = 2 s, post-labeling delay = 1,900 ms (15). The labeling plane was 6 cm apart from the imaging slice, proximally for the tag scan and distally for the control (15).

An ischemic-hyperemic paradigm was chosen to create a uniform challenge across all muscle groups and across all subjects. A Zimmer 1000 (Warsaw, Indiana) nonmagnetic tourniquet system, with thigh cuff, was used to create a 5-min period of ischemia at 250 mm Hg, followed by a period of hyperemic flow. The CASL imaging commenced upon cuff inflation and ended 3 min after cuff deflation. A 2-dimensional spoiled gradient-echo sequence (repetition time/echo time = 50/3.4 ms, field-of-view = 220 mm, in-plane matrix size = 256 × 256, flip angle = 50°, with 4 averages) was used to acquire a high-resolution anatomic image of the slice where CASL imaging was performed.

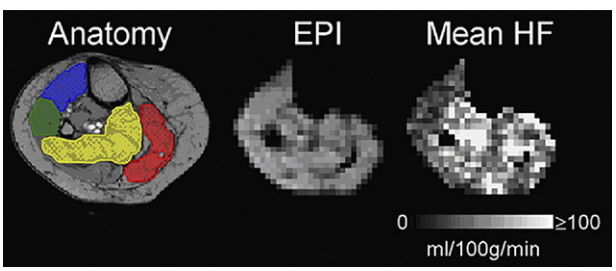

Figure 1 **Cross-Sectional Images of the Mid-Calf in a Representative Subject**

High-resolution anatomic image **(left)**, echo-planar (EPI) image **(middle)**, and mean hyperemic flow (HF) map **(right)**. The regions of interest for anterior compartment **(blue)**, lateral compartment **(green)**, soleus muscle **(yellow)**, and medial gastrocnemius **(red)** are overlaid on the anatomic image. Mean HF is the average flow during the hyperemic period.

Abbreviations and Acronyms

ABI = ankle-to-brachial index
ASL = arterial spin labeling
CASL = continuous arterial spin-labeling
GstrcM = gastrocnemius muscle
MRI = magnetic resonance imaging
PAD = peripheral arterial disease
PHF = peak hyperemic flow
SolM = soleus muscle
T1 = longitudinal relaxation time constant
T2 = transverse relaxation time constant
TTP = time-to-peak

Data processing and image analysis. Reconstructed magnitude images were analyzed offline with VoxBo (19) and IDL (RSI, Boulder, Colorado). The CASL signals were generated by pair-wise subtraction of tag and control images, and 2 adjacent data points in time were averaged, resulting in an effective temporal resolution of 16 s. The CASL signal (Delta M) was then converted to quantitative flow (f) in ml/100 g/min:

$$f = \frac{\lambda \Delta M}{2\alpha T_1 M_0 \left[\exp\left(-\frac{PLD}{T_1}\right) - \exp\left(-\frac{PLD+\tau}{T_1}\right)\right]} \quad [1]$$

where M_0 is the fully-relaxed blood signal, α is the tagging efficiency (0.80), PLD is the post-labeling delay, and τ is the tagging duration (20). We assumed that $T_1/T_2^* = 1{,}600/100$ ms for arterial blood at 3.0-T and the blood/tissue partition coefficient (λ) = 0.9 ml/g, comparable to the value measured in the brain (21). For further details regarding the model, please refer to Wu et al. (16).

Four muscle groups in the mid-calf were analyzed, representing the vascular distributions of the 3 major branches of the popliteal artery. The soleus muscle (SolM) receives a dual vascular supply from both the posterior tibial and the peroneal arteries. The medial gastrocnemius muscle (GstrcM) is supplied by the posterior tibial artery. The anterior compartment contains extensor muscles, including the extensor digitorum longus, extensor hallicus longus, tibialis anterior, and peroneus muscles, and is supplied by the anterior tibial artery. Finally, the lateral compartment contains the peroneus longus and peroneus brevis muscles, and is supplied by the peroneal artery. Regions of interest were hand-drawn on the high-resolution spoiled gradient-echo anatomic images (Fig. 1). Two flow indexes were computed as defined in the following (Fig. 2):

1. Peak hyperemic flow (PHF) (ml/100 g/min): the peak flow observed in hyperemic period, which spans from the time (t_{beg}) when flow increases above a threshold (f_T) to the time (t_{end}) when flow returns to f_T. Here, t_{beg} is later

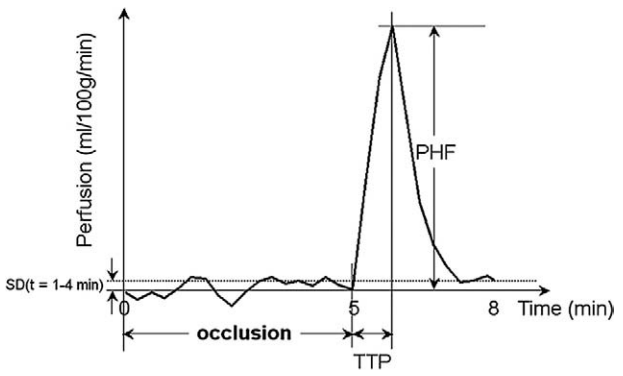

Figure 2 Schematic Illustration of the Ischemic-Hyperemic Paradigm and the Flow Indexes Measured in This Study

PHF = peak hyperemic flow; TTP = time-to-peak.

than the time of cuff deflation, and f_T is chosen to be 1 SD of the "flow" during the center 3-min occlusion when ideally flow is 0.

2. Time-to-peak (TTP) (s): measured from the time when cuff is deflated to the time when hyperemic flow peaks.

Statistical analysis. A random effects model (22) was employed to test the dependence of PHF upon the variables muscle group and ABI as well as for any interaction effects between muscle group and ABI (muscle × ABI). Because TTP was a count of the number of 16-s epochs and followed a Poisson distribution, the TTP measure was modeled with generalized estimating equations (23) with a Poisson family assumption. The ABI was treated as a continuous measure in all analyses.

Results

Table 1 gives a breakdown of demographic data for the population studied by ABI category. Overall, the groups are well-balanced by age, disease characteristics, and sex. The relatively fewer number of subjects in category 3 reflects the decreased frequency of PAD of this severity and the difficulty of enrolling subjects with more severe disease.

Table 2 offers a breakdown of mean ± SD measurements for PHF and TTP by muscle group and ABI category. In Figure 3, the average of subjects' individual flow-time curves is plotted for different muscle groups as well as the PAD stages defined by ABI. Qualitatively it can be seen that with increasing disease severity, PHF decreases, TTP increases, and the hyperemic period is broadened. Figure 4 graphs both mean TTP and PHF by ABI category and muscle group. From Table 2 and Figures 3 and 4, there is evidence of a fall in PHF in all muscle groups with increasing disease severity, as reflected in the ABI category. For SolM, the decrease in PHF seems to be delayed until category 3. In contrast, the TTP increase in response to increasing disease severity seems to occur in a nearly parallel fashion for all muscle groups. Thus, for most muscle groups, falling PHF as well as increasing TTP occur with early stages of disease; yet uniquely for SolM, increasing TTP might be a more sensitive indicator of early vascular disease.

Shown in Figure 5 is a scatter-plot with mean TTP versus mean PHF. The data show that TTP is inversely associated with PHF. The TTP of 60 s in combination with PHF of 63 ml/100 g/min provides an approximate demarcation between categories 0 to 1 and 2 to 3, with an exception of category 2 SolM (see the arrow). This might indicate somewhat better flow preservation with severe PAD in SolM than in other muscle groups.

Statistical analysis of the dependence of PHF and TTP upon ABI and muscle groups is summarized in Tables 3 and 4, respectively. The PHF was dependent upon muscle group

Table 2 Summary of Measured Flow Indexes

Muscle Groups/ Categories		Flow Indexes: Peak Hyperemic Flow (ml/100 g/min)	Flow Indexes: Time-To-Peak (s)
SolM	0	91 ± 39	47 ± 12
	1	97 ± 47	54 ± 13
	2	100 ± 48	68 ± 21
	3	60 ± 13	77 ± 26
GstrcM	0	71 ± 42	53 ± 18
	1	69 ± 27	57 ± 19
	2	61 ± 33	71 ± 26
	3	50 ± 17	88 ± 38
AC	0	71 ± 28	45 ± 8
	1	80 ± 44	49 ± 15
	2	55 ± 19	65 ± 24
	3	53 ±20	86 ± 51
LC	0	67 ± 41	55 ± 23
	1	66 ± 35	56 ± 15
	2	51 ± 28	76 ± 29
	3	44 ± 19	99 ± 38

Values expressed as mean ± SD.
AC = anterior compartment; GstrcM = medial head of gastrocnemius; LC = lateral compartment; SolM = soleus muscle.

Table 1 Demographic Summary of the Patients Recruited in This Study

ABI	Category	n	Sex (F/M)	Age (yrs)	DM	HTN	Smoking
0.9 ≤ ABI ≤1.3	0	17	6/11	59 ± 15	5	9	5
0.7 ≤ ABI <0.9	1	17	8/9	65 ± 15	8	13	9
0.5 ≤ ABI <0.7	2	16	7/9	60 ± 14	7	12	8
ABI <0.5	3	7	3/4	62 ± 17	4	4	5

ABI = ankle-to-brachial index; DM = diabetes mellitus; HTN = hypertension.

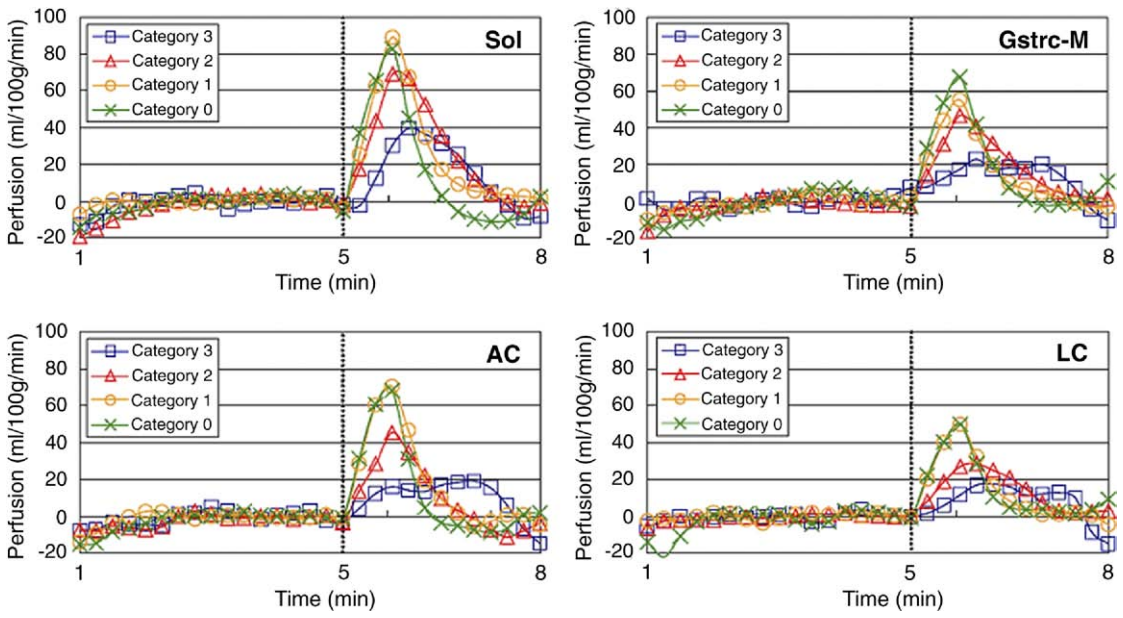

Figure 3 Perfusion-Time Curves for Different Muscles and Categories of the Ankle-to-Brachial Index

Vertical dotted lines indicate the time when cuff is released. AC = anterior compartment; GstrcM = medial head of gastrocnemius; LC = lateral compartment; SolM = soleus muscle.

($p < 0.0001$) and ABI ($p = 0.04$). Within the muscle groups studied, PHF for SolM demonstrated relative resistance (coefficient = 26, $p < 0.0001$), and lateral compartment demonstrated relatively greater sensitivity (coefficient = −14, $p < 0.0001$) to the effect of increasing ABI, all relative to the GstrcM reference group. The TTP was found to be dependent upon both muscle group ($p = 0.001$) and ABI ($p < 0.0001$), with TTP increasing with increasing severity of disease. Although TTP was dependent upon muscle group, only anterior compartment seemed to demonstrate significant deviation in the behavior of TTP from the reference GstrcM group.

Discussion

Peripheral artery disease is usually associated with discrete lesions within 1 or several vessels. The traditional understanding of PAD is one of progressive blood flow impair-

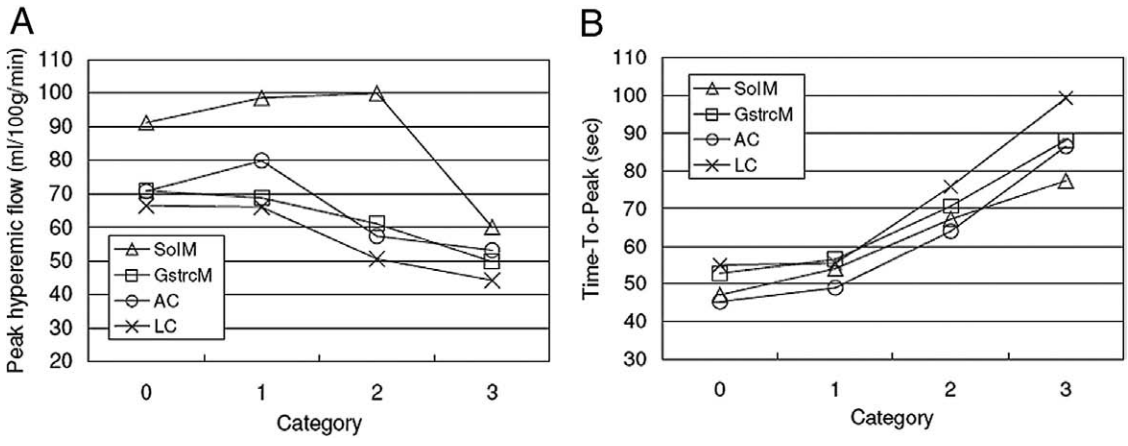

Figure 4 Relationship Between Flow Indexes, Muscle Group, and Disease Category

Flow indexes: **(A)** peak hyperemic flow, **(B)** time-to-peak. Two main effects: "muscle group" and "category" (disease severity assessed by the ankle-to-brachial index). Abbreviations as in Figure 3.

JACC Vol. 53, No. 25, 2009
June 23, 2009:2372–7

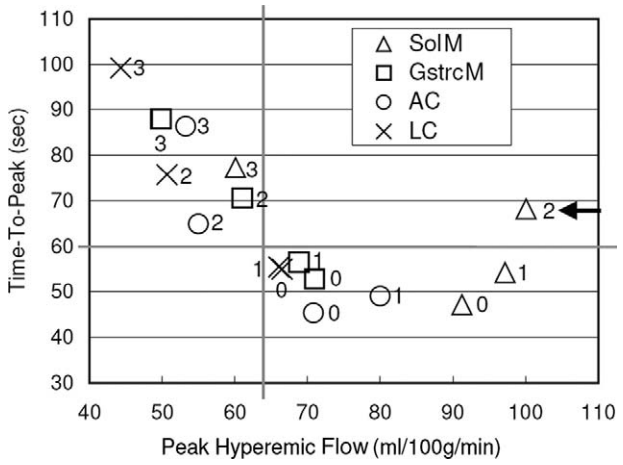

Figure 5 Relationship Between Time-to-Peak and Peak Hyperemic Flow

Muscle groups are denoted by mark styles (**triangle**: SolM, **square**: GstrcM, **circle**: AC, **cross**: LC). Categories (peripheral arterial disease stages) are numerically labeled. Abbreviations as in Figure 3.

ment in conduit vessels that, through the creation of chronic ischemic environment, ultimately affects the end organ, skeletal muscle (2). Whereas arterial supply varies between muscle groups, flow heterogeneity between muscle groups is thought to be a consequence of different composition of myofibril type and/or metabolic profile (7,16). Therefore it is conceivable that muscle groups might be differentially affected by PAD.

In the present study, we measured 2 indexes of post-ischemic reactive hyperemia, PHF and TTP, in healthy subjects and in subjects with a range of PAD with a completely noninvasive MRI methodology, CASL. The PHF was noted to decrease and TTP to increase with decreasing ABI and in conjunction with increasing PAD severity. Whereas TTP seems to respond almost immediately to PAD progression, PHF is relatively well-preserved until subjects fall into cateogory 2 and seems to be preserved even longer in the SolM.

Table 3 Summarized Statistical Results of the Dependence of PHF Upon Muscle Group and ABI

Factor	Coefficient Est	SEM	p Value
Intercept	43	14	0.0044
SolM	26	2.7	<0.0001
AC	−4.3	2.8	0.13
LC	−14	2.9	<0.0001
Muscle group	—	—	<0.0001
ABI	36	17	0.04

A random effects model was used. The interaction between muscle group and peak hyperemic flow (PHF) was not found to be significant ($R^2 = 0.73$, $p = 0.99$). Within the muscle groups studied, PHF sensitivity to the effect of increasing ankle-to-brachial index (ABI) was tested relative to the reference group medial head of gastrocnemius (GstrcM). Negative coefficients (anterior compartment [AC] and lateral compartment [LC]) indicate relatively greater sensitivity, whereas positive coefficients (soleus muscle [SolM]) indicate relatively greater resistance of PHF within these individual muscle groups to increasing severity of disease.

Table 4 Summarized Statistical Results of the Dependence of TTP Upon Muscle Group and ABI

Factor	Coefficient Est	SEM	p Value
SolM	0.92	0.04	0.079
AC	0.88	0.06	0.049
LC	1.1	0.06	0.34
Muscle group	—	—	0.001
ABI	0.4	0.075	<0.0001

Generalized estimating equations were used. Within the muscle groups studied, time-to-peak (TTP) sensitivity to the effect of increasing ABI was tested relative to the reference group GstrcM. Although TTP was found to depend upon muscle group, only AC demonstrated significant deviation in the behavior of TTP from the reference GstrcM group.

Abbreviations as in Table 3.

We and others have previously demonstrated that PHF is higher in SolM than in all other calf muscle groups at baseline in healthy subjects (8,16). However, the relative resilience of hyperemic flow to advancing PAD in SolM, as compared with other muscle groups, is revealed for the first time. SolM is composed of approximately 70% to 80% slow-twitch type I fibers with a higher capillarity and oxidative capacity, which enables SolM to convert and use energy more effectively and thus better endure insufficient supply of flow, oxygen, and nutrients accompanying disease progression (i.e., greater resistance to hypoxia). By contrast, gastrocnemius is more evenly composed of type I (50% to 60%) and type II fibers. Myofibril composition and differences in metabolic profiles might also account for the relative resistance of the SolM to the presence of PAD.

We also observed an early prolongation in TTP with disease progression that increased in a parallel fashion amongst all the muscle groups studied (Fig. 4B). This greater similarity in behavior of TTP across muscle groups is not surprising in that we have previously demonstrated that TTP is independent of muscle group (16). We also found an inverse correlation between TTP and PHF (Fig. 5). Although TTP increased early in disease, PHF did not decrease immediately, suggesting that microvascular reactivity partially compensates early on for the narrowing in large feeding vessels. In comparison with PHF, TTP seems more sensitive to early disease progression. A combination of the 2 flow indexes might offer more comprehensive information for the grading and/or diagnosis of PAD.

Conclusions

CASL flow measurements correlate with disease state as measured by ABI and demonstrate preserved microvascular flow reserve in the presence of early-to-intermediate vascular disease (categories 0 to 2). Changes in the ABI, an indirect measure of large vessel stenosis, tracks closely with TTP, preceding perfusion changes, and appears to be countered by a preserved microvascular flow reserve until late stage in disease progression. The ASL approach might have several unique properties in the diagnosis and study of PAD, offering an extrinsic "contrast free" approach to assess

end-organ microvascular results of chronic disease and therapy.

Acknowledgments

The authors thank Temitope Olufade, BS, MPH, for research coordination; Jiongjiong Wang, PHD for technical consultation; and Lee J. Milas, BS, for assisting with data acquisition.

Reprint requests and correspondence: Dr. Thomas F. Floyd, Departments of Neurology and Anesthesiology & Critical Care, The Hospital of University of Pennsylvania, 3400 Spruce Street, Philadelphia, Pennsylvania 19104. E-mail: Thomas.Floyd@uphs.upenn.edu.

REFERENCES

1. Mohler ER III. Peripheral arterial disease: identification and implications. Arch Intern Med 2003;163:2306–14.
2. Bragadeesh T, Sari I, Pascotto M, Micari A, Kaul S, Lindner JR. Detection of peripheral vascular stenosis by assessing skeletal muscle flow reserve. J Am Coll Cardiol 2005;45:780–5.
3. Isbell DC, Berr SS, Toledano AY, et al. Delayed calf muscle phosphocreatine recovery after exercise identifies peripheral arterial disease. J Am Coll Cardiol 2006;47:2289–95.
4. Davidson SM, Duchen MR. Endothelial mitochondria: contributing to vascular function and disease. Circ Res 2007;100:1128–41.
5. Bosch-Marce M, Okuyama H, Wesley JB, et al. Effects of aging and hypoxia-inducible factor-1 activity on angiogenic cell mobilization and recovery of perfusion after limb ischemia. Circ Res 2007;101:1310–8.
6. Mitchell RG, Duscha BD, Robbins JL, et al. Increased levels of apoptosis in gastrocnemius skeletal muscle in patients with peripheral arterial disease. Vasc Med 2007;12:285–90.
7. Kalliokoski KK, Kemppainen J, Larmola K, et al. Muscle blood flow and flow heterogeneity during exercise studied with positron emission tomography in humans. Eur J Appl Physiol 2000;83:395–401.
8. Thompson RB, Aviles RJ, Faranesh AZ, et al. Measurement of skeletal muscle perfusion during postischemic reactive hyperemia using contrast-enhanced MRI with a step-input function. Magn Reson Med 2005;54:289–98.
9. Weber MA, Jappe U, Essig M, et al. Contrast-enhanced ultrasound in dermatomyositis- and polymyositis. J Neurol 2006;253:1625–32.
10. Detre JA, Leigh JS, Williams DS, Koretsky AP. Perfusion imaging. Magn Reson Med 1992;23:37–45.
11. Laughlin MH, Korthuis RJ, Sexton WL, Armstrong RB. Regional muscle blood flow capacity and exercise hyperemia in high-intensity trained rats. J Appl Physiol 1988;64:2420–7.
12. Pohmann R, Kunnecke B, Fingerle J, von Kienlin M. Fast perfusion measurements in rat skeletal muscle at rest and during exercise with single-voxel FAIR (flow-sensitive alternating inversion recovery). Magn Reson Med 2006;55:108–15.
13. Lebon V, Carlier PG, Brillault-Salvat C, Leroy-Willig A. Simultaneous measurement of perfusion and oxygenation changes using a multiple gradient-echo sequence: application to human muscle study. Magn Reson Imaging 1998;16:721–9.
14. Frank LR, Wong EC, Haseler LJ, Buxton RB. Dynamic imaging of perfusion in human skeletal muscle during exercise with arterial spin labeling. Magn Reson Med 1999;42:258–67.
15. Wu WC, Wang J, Detre JA, Ratcliffe SJ, Floyd TF. Transit delay and flow quantification in muscle with continuous arterial spin labeling perfusion-MRI. J Magn Reson Imaging 2008;28:445–52.
16. Wu WC, Wang J, Detre JA, et al. Hyperemic flow heterogeneity within the calf, foot, and forearm measured with continuous arterial spin labeling MRI. Am J Physiol Heart Circ Physiol 2008;294:H2129–36.
17. Hiatt WR. Medical treatment of peripheral arterial disease and claudication. N Engl J Med 2001;344:1608–21.
18. Alsop DC, Detre JA. Reduced transit-time sensitivity in noninvasive magnetic resonance imaging of human cerebral blood flow. J Cereb Blood Flow Metab 1996;16:1236–49.
19. VoxBoWiki. Available at: http://www.voxbo.org/. Accessed May 15, 2009.
20. Roberts DA, Detre JA, Bolinger L, Insko EK, Leigh JS Jr. Quantitative magnetic resonance imaging of human brain perfusion at 1.5 T using steady-state inversion of arterial water. Proc Natl Acad Sci U S A 1994;91:33–7.
21. Herscovitch P, Raichle ME. What is the correct value for the brain–blood partition coefficient for water? J Cereb Blood Flow Metab 1985;5:65–9.
22. Laird NM, Ware JH. Random-effects models for longitudinal data. Biometrics 1982;38:963–74.
23. Zeger SL, Liang KY. Longitudinal data analysis using generalized linear models. Biometricka 1986;73:13–22.

Key Words: arterial spin-labeling ■ magnetic resonance imaging ■ peripheral arterial disease ■ skeletal muscle.